

## Electronic Supplementary Information

### **Copper (I) sulfide: A two-dimensional semiconductor with superior oxidation resistance and high carrier mobility**

Yu Guo,<sup>ab</sup> Qisheng Wu,<sup>bc</sup> Yunhai Li,<sup>c</sup> Ning Lu,<sup>d</sup> Keke Mao,<sup>be</sup> Yizhen Bai,<sup>a</sup> Jijun Zhao,<sup>\*a</sup> Jinlan Wang<sup>\*cf</sup> and Xiao Cheng Zeng<sup>\*bg</sup>

<sup>a</sup>*Key Laboratory of Materials Modification by Laser, Ion and Electron Beams (Dalian University of Technology), Ministry of Education, Dalian, Liaoning 116024, China*

<sup>b</sup>*Department of Chemistry, University of Nebraska–Lincoln, Lincoln, Nebraska 68588, United States*

<sup>c</sup>*School of Physics, Southeast University, Nanjing, Jiangsu 211189, China*

<sup>d</sup>*Anhui Province Key Laboratory of Optoelectric Materials Science and Technology, Department of Physics, Anhui Normal University, Wuhu, Anhui 241000, China*

<sup>e</sup>*School of Energy and Environment Science, Anhui University of Technology, Maanshan, Anhui 243032, China*

<sup>f</sup>*Synergetic Innovation Center for Quantum Effects and Applications (SICQEA), Hunan Normal University, Changsha, Hunan 410081, China*

<sup>g</sup>*Department of Chemical & Biomolecular Engineering and Department of Mechanical & Materials Engineering, University of Nebraska–Lincoln, Lincoln, Nebraska 68588, United States*

---

\*Corresponding authors: zhaojj@dlut.edu.cn (J. Zhao); jlwang@seu.edu.cn (J. Wang); xzeng1@unl.edu (X. C. Zeng)

## S1. Geometric structures, dynamical and thermal stability of selected Cu<sub>2</sub>S monolayers

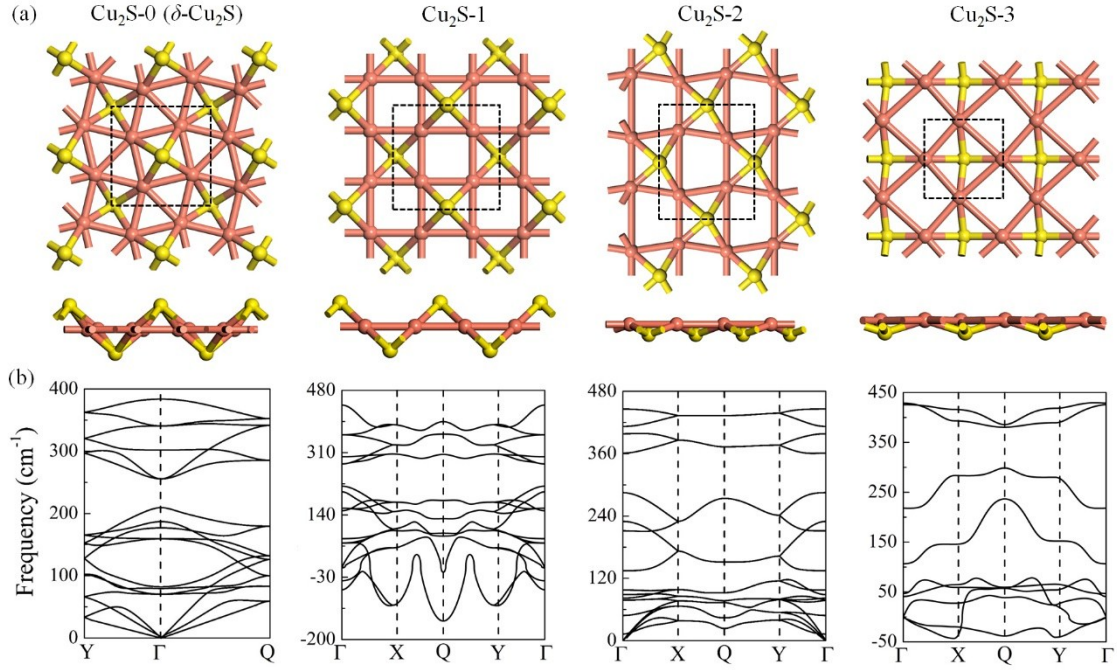


**Fig. S1.** (a) Four representative low-energy structures of freestanding Cu<sub>2</sub>S monolayer predicted by using the CALYPSO code. The unit cells are denoted by dashed lines. Cu and S atoms are shown in pink and yellow, respectively. (b) Corresponding phonon dispersions of the four polymorph structures. High-symmetry points of the first Brillouin zone are:  $\Gamma$  (0, 0, 0), X (0.5, 0, 0), Y (0, 0.5, 0) and Q (0.5, 0.5, 0). Among four structures, only Cu<sub>2</sub>S-0 ( $\delta$ -Cu<sub>2</sub>S) and Cu<sub>2</sub>S-2 are dynamically stable.

**Table S1.** Formation energies ( $\Delta H$ ) of four Cu<sub>2</sub>S monolayer structures shown in Fig. S1.

System	Cu <sub>2</sub> S-0 ( $\delta$ -Cu <sub>2</sub> S)	Cu <sub>2</sub> S-1	Cu <sub>2</sub> S-2	Cu <sub>2</sub> S-3
$\Delta H$ (eV/atom)	-0.21	-0.13	0.05	0.07

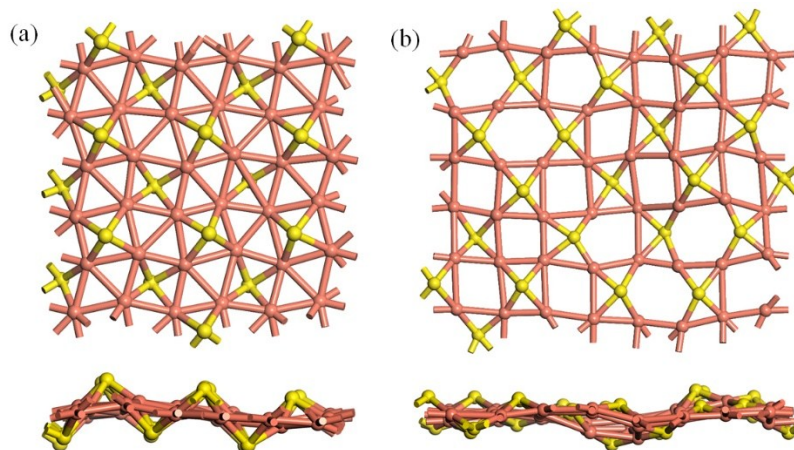


**Fig. S2.** Snapshots structures of the  $\delta$ -Cu<sub>2</sub>S (a) and Cu<sub>2</sub>S-2 monolayers (b) after 10 ps Born-Oppenheimer molecular dynamic simulations, with the temperature being controlled at 300 K. Cu and S atoms are shown in pink and yellow, respectively.

## S2. Geometric and electronic structures of $\beta$ -Cu<sub>2</sub>S bilayer

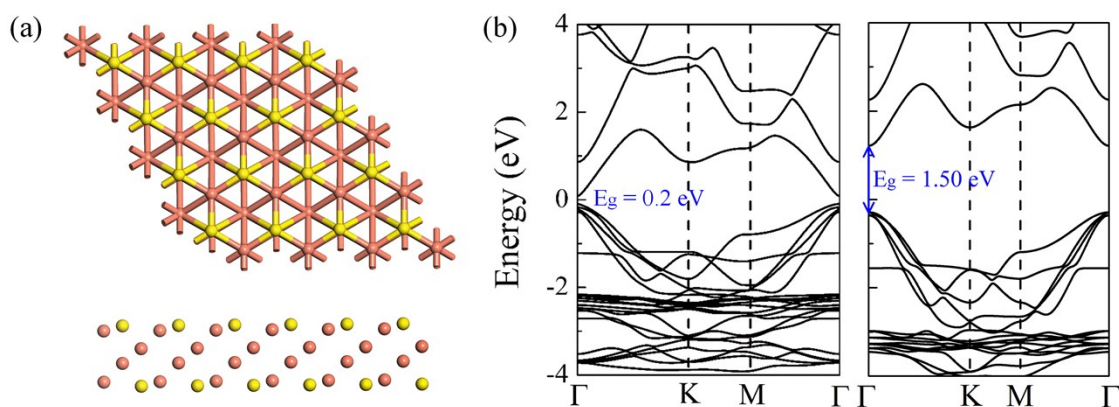


**Fig. S3.** (a) Top and side views of the experimentally fabricated  $\beta$ -Cu<sub>2</sub>S bilayer (see *Adv. Mater.* **2016**, 28, 8271–8276). (b) Band structure of  $\beta$ -Cu<sub>2</sub>S bilayer with a direct band gap ( $E_g$ ) at  $\Gamma$  point, computed based on PBE (left panel) and HSE06 level (right panel), respectively. The Fermi level is set to zero.

**S3. Snapshots of  $\delta$ -Cu<sub>2</sub>S monolayer taken at the end of each Born-Oppenheimer molecular dynamics (BOMD) simulation**

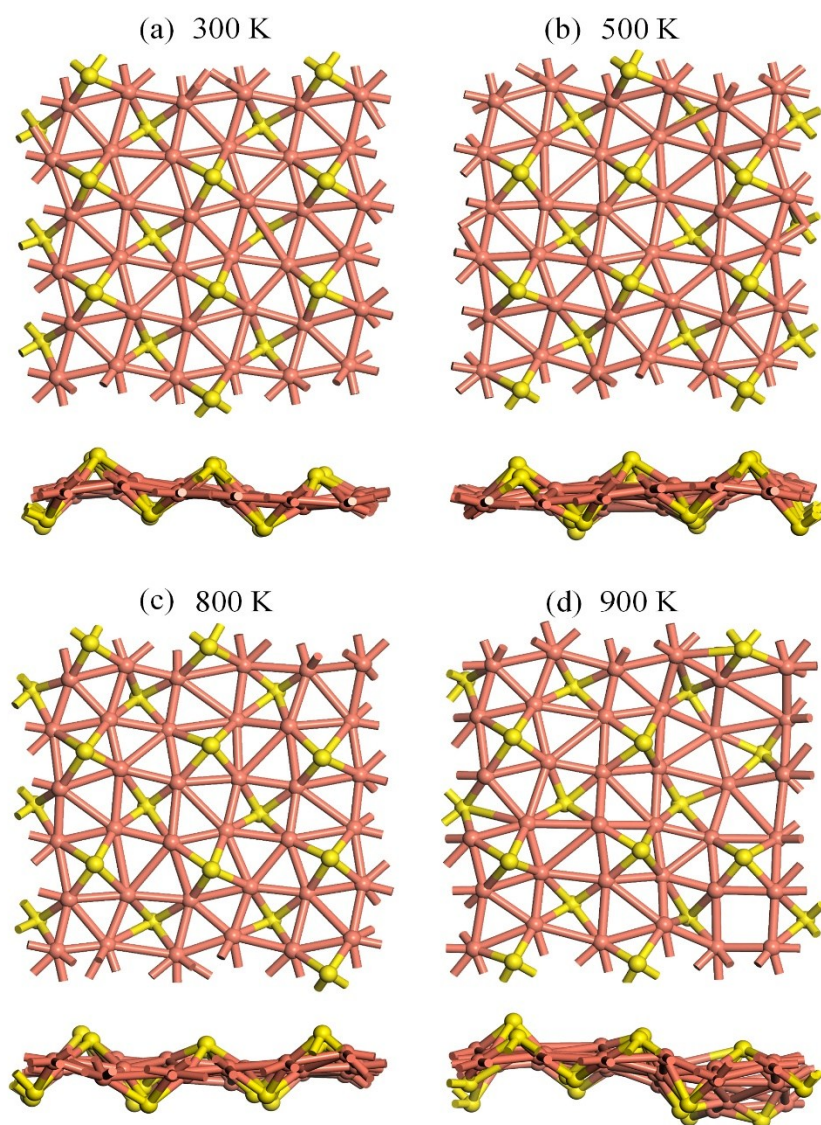


**Fig. S4.** Structure snapshots of  $\delta$ -Cu<sub>2</sub>S monolayer from BOMD simulations with temperature being controlled at (a) 300, (b) 500, (c) 800, and (d) 900 K, respectively. Each simulation lasts for 10 ps.



#### S4. Several adsorption sites for O<sub>2</sub> on $\delta$ -Cu<sub>2</sub>S

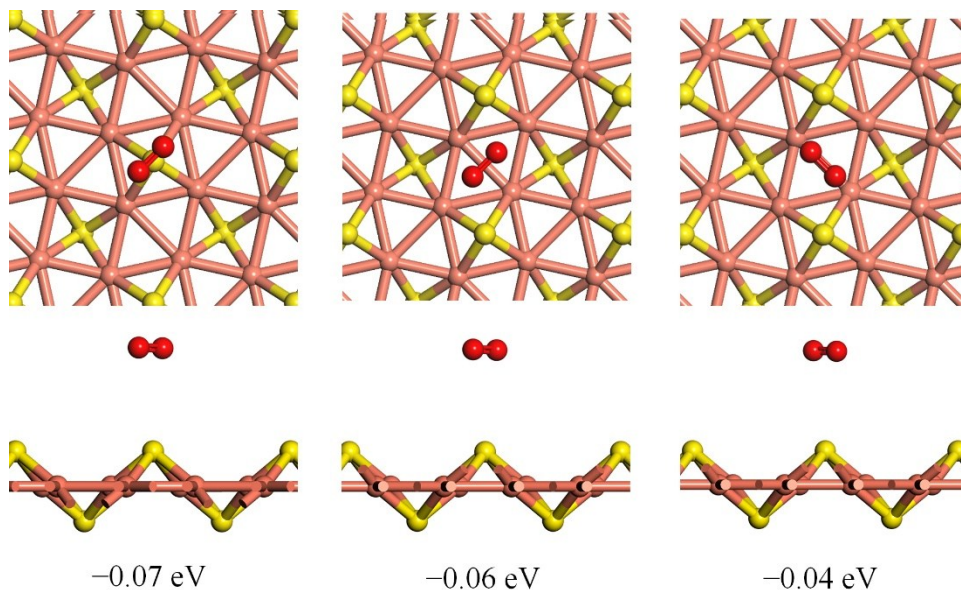


**Fig. S5.** Top and side views of local geometries for several other adsorption sites for O<sub>2</sub>. The number at the bottom indicate the binding energy of O<sub>2</sub> adsorption on  $\delta$ -Cu<sub>2</sub>S. Since O<sub>2</sub> chemisorption on  $\delta$ -Cu<sub>2</sub>S exhibits only one configuration (see Fig. 3), the structures of O<sub>2</sub> physisorbed on  $\delta$ -Cu<sub>2</sub>S are shown here.

#### S5. Chemical stability of $\delta$ -Cu<sub>2</sub>S monolayer considering experimental O<sub>2</sub> bonding energy

**Table S2.** A comparison of energies for initial ( $E^i$ ), transition ( $E^t$ ) and final ( $E^f$ ) states, activation energy ( $E^a$ ), and heat of reaction ( $E^H$ ) with either the experimental or DFT calculated O<sub>2</sub> bonding energy as the reference. The unit of  $E^i$ ,  $E^t$ ,  $E^f$ ,  $E^a$  and  $E^H$  is eV.

	$E^i$	$E^t$	$E^f$	$E^a$	$E^H$
Exp.	-1.74	0.24	-1.82	1.98	0.08
DFT	-0.09	1.89	-0.17	1.98	0.08

### S6. BOMD simulations of O<sub>2</sub> collision with $\delta$ -Cu<sub>2</sub>S monolayer at 300 K

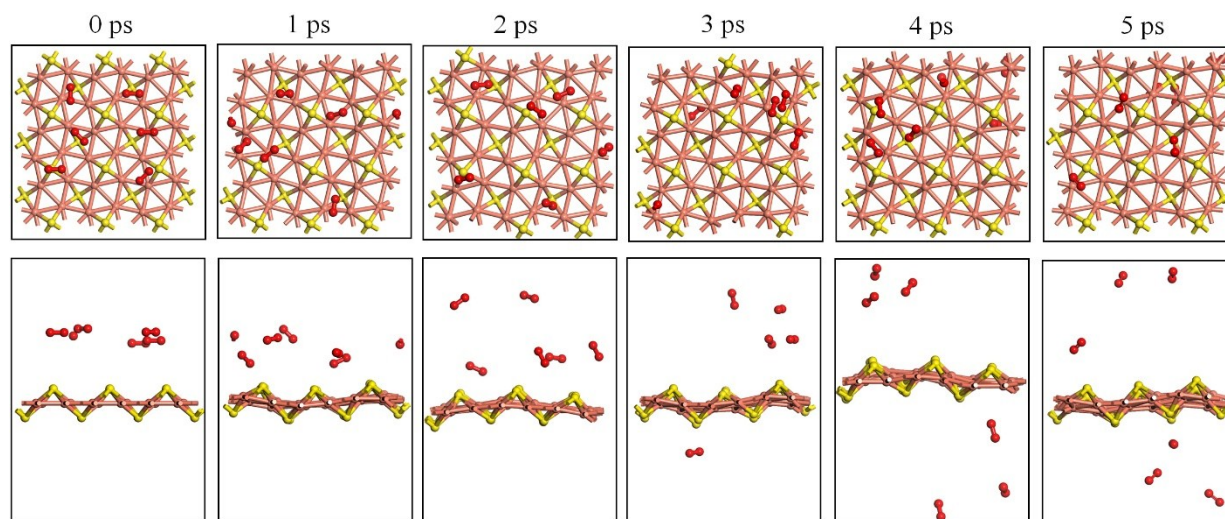


**Fig. S6.** Snapshots of BOMD simulations of O<sub>2</sub> oxidation at 300 K at 1 - 5 ps. It can be seen that O<sub>2</sub> molecules are typically bounced back to the vacuum after collision with the  $\delta$ -Cu<sub>2</sub>S monolayer. Hence, it seems that  $\delta$ -Cu<sub>2</sub>S monolayer exhibits superior oxidation resistance.

### S7. Strain effect on the band structure of $\delta$ -Cu<sub>2</sub>S monolayer

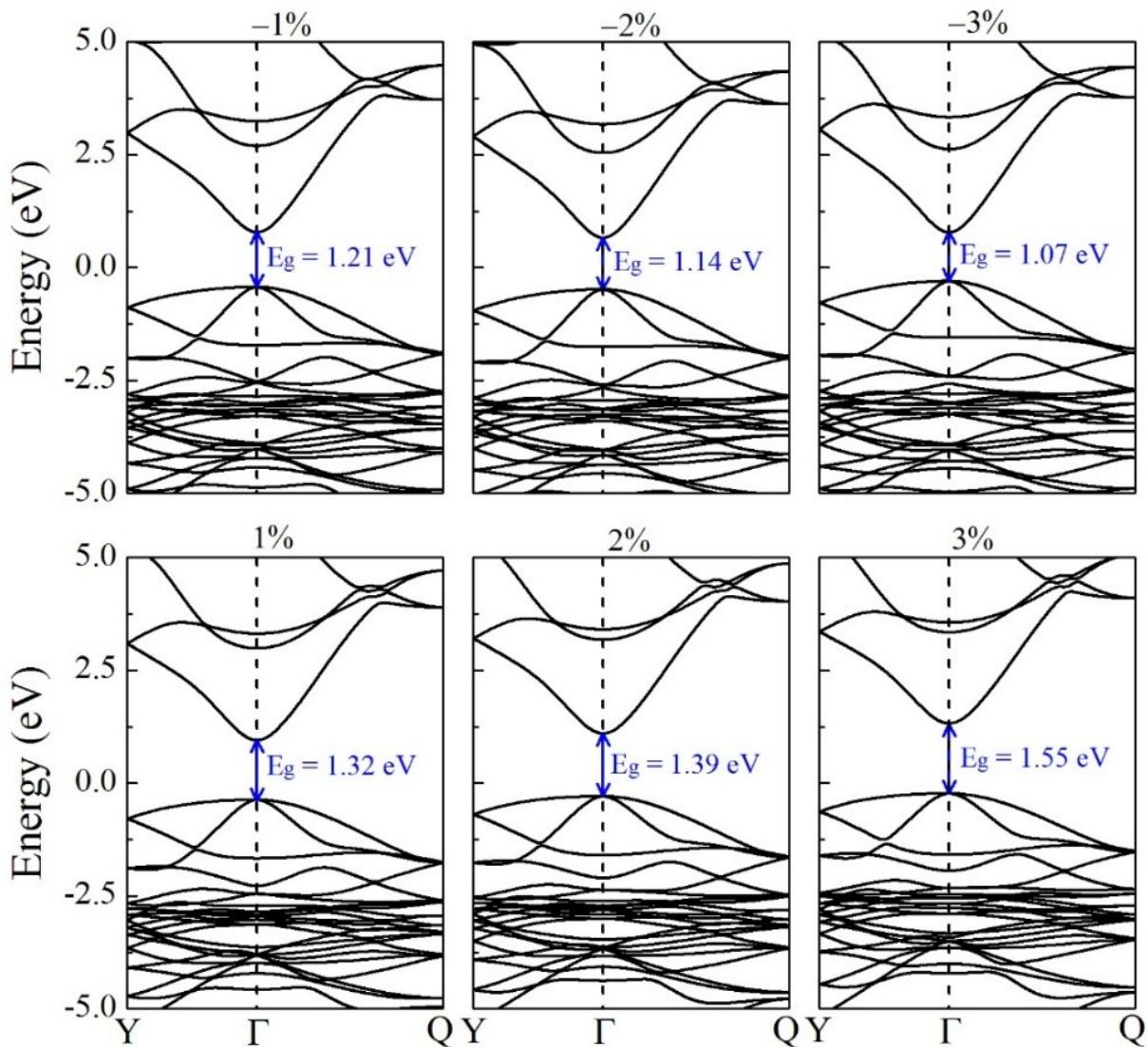


**Fig. S7.** Band structures of  $\delta$ -Cu<sub>2</sub>S monolayer under various lateral strain from  $-3\%$  to  $3\%$ , computed based on HSE06 functional. Fermi levels are set to zero.  $E_g$  is the band gap denoted by the solid arrow.

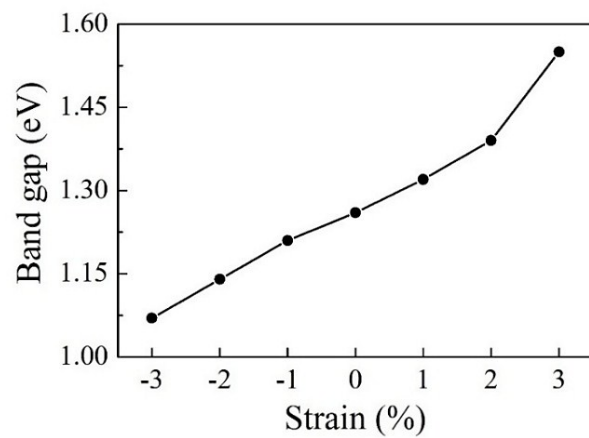


**Fig. S8.** Strain effect on the band gap of  $\delta$ -Cu<sub>2</sub>S monolayer calculated based on the HSE06 functional.